Line-field confocal optical coherence tomography (LC-OCT): principles and practical use

Jonas Ogien, Clara Tavernier, Sébastien Fischman, Arnaud Dubois

Line-field confocal optical coherence tomography (LC-OCT): principles and practical use

Jonas OGIEN [1] *, Clara TAVERNIER [1], Sébastien FISCHMAN [1], Arnaud DUBOIS [1,2]

[1]DAMAE Medical, Paris, France; [2]Laboratoire Charles Fabry, Institut d'Optique Graduate School, Paris-Saclay University, Palaiseau, France

*Corresponding author: Jonas Ogien, DAMAE Medical, 14 rue Sthrau 75013 Paris, France. E-mail: jonas@damae-medical.com

ABSTRACT

Line-field confocal optical coherence tomography (LC-OCT) is a non-invasive optical imaging technique based on a combination of the optical principles of optical coherence tomography and reflectance confocal microscopy with line-field illumination, which can generate cell-resolved images of the skin, *in vivo*, in vertical section, horizontal section and in three dimensions. This article reviews the optical principles of LC-OCT, including low coherence interferometry, confocal filtering and line-field arrangement. The optical setup allowing for the acquisition of color images of the skin surface in parallel with LC-OCT images, without compromising LC-OCT performance, is also presented. Practical use of LC-OCT is demonstrated through an overview of the workflow of examining a patient using a commercial handheld LC-OCT probe (deepLive™, DAMAE Medical), from creating the patient record in the software, acquiring the images, to reviewing and interpreting the images. LC-OCT can generate a significant amount of data, making automated deep learning algorithms particularly relevant for assisting in the analysis of LC-OCT images. A review of algorithms developed for skin layer segmentation, keratinocyte nuclei segmentation, and automatic detection of atypical keratinocyte nuclei is provided.

(*Cite this article as:* Ogien J, Tavernier C, Fischman S, Dubois A. Line-field confocal optical coherence tomography (LC-OCT): principles and practical use. Ital J Dermatol Venereol 2023;158:171-9. DOI: 10.23736/S2784-8671.23.07613-2)

KEY WORDS: Optical coherence tomography; Confocal microscopy; Optical imaging.

Non-invasive optical imaging is a valuable tool in dermatology, specifically for the diagnosis, mapping and monitoring of skin diseases. In particular, dermoscopy has become a standard tool in dermatological practice,[1] as it allows high resolution examination of the skin surface, offering the possibility to observe relevant features of lesions otherwise not visible to the naked eye. Nevertheless, diagnostic accuracy of dermoscopy is dependent upon the degree of experience of the examiner,[2] and histological examination of the skin remains the gold standard for diagnosing skin diseases, especially for skin cancer. Histology is generally performed on slices of tissue obtained from a biopsy, after preparation and using conventional white light microscopy. This process requires an invasive procedure, and the resulting images can rarely be obtained in real time due to the necessary preparation of the sample, yielding a delay between the biopsy and the examination results, and making it complicated to monitor and map lesions, particularly during surgery. Therefore, non-invasive optical imaging techniques allowing for "*in vivo* histology" by providing cellular resolution images in depth within the skin non-invasively could yield real-time diagnosis, which would enable rapid management, while also reducing the number of biopsies and giving the possibility to improve lesion monitoring and mapping during surgery and follow-up examination.

To date, the main technique used routinely for non-invasive cellular level imaging of skin tissue is reflectance confocal microscopy (RCM).[3] RCM generates horizontal (en face) sections of the skin up to a depth of 200-300 microns, giving access to features at the scale of histology. The use of RCM has been shown to be able to significantly reduce the number of needed biopsies in skin cancer management,

in particular for melanocytic lesions.[4] However, RCM images are fundamentally different from conventional histology images, which are vertical sections, showing the different layers of the skin. This complicates the image interpretation for non-experienced users, and is not well suited for the diagnosis of certain diseases.[5] Furthermore, the clinical relevance of RCM has been shown mainly for a particular implementation generating mosaic images, covering a large field of view (8 × 8 mm²),[4, 6] but requiring an adapter to be positioned on the skin,[7] complicating its use on non-flat skin surfaces, especially on the face.

Line-field confocal optical coherence tomography (LC-OCT) was introduced in 2018 as a non-invasive optical imaging technique allowing generation of real-time cellular level vertical section images comparable to conventional histology images,[8] with an improved penetration depth compared to RCM.[9] Since then, LC-OCT has been improved with new imaging modes, allowing for this technology to generate not only vertical section images, but also horizontal section images similar to RCM images[10] and three-dimensional (3D) images.[11] LC-OCT systems have been miniaturized to fit within ergonomic handheld probes allowing for an easy access of any skin area on the body.[11, 12] Eventually, an optical system providing a guiding image of the surface of the skin at a dermoscopic scale was integrated to LC-OCT, allowing for a precise positioning of the cellular level acquisition, without compromising the ergonomics of the probe.[13] The interest of the technique for the early diagnosis and the therapeutic follow-up of numerous skin diseases, in particular cancerous lesions, has been demonstrated.[14-18]

In this article, we will first outline the optical principles of the most recent LC-OCT implementation. Details will be given on the optical setup allowing for LC-OCT imaging with guiding image acquisition. A second part will cover the different imaging modes offered by this implementation, with corresponding performance in terms of resolution, field of view and acquisition speed, illustrated by examples of skin images. Then, the focus will be on the practical use of a commercial handheld LC-OCT probe (deepLive™, DAMAE Medical), from creating the patient record in the software, acquiring the images, to reviewing and interpreting the images. Eventually, newly developed artificial intelligence algorithms for improving LC-OCT image analysis will be introduced.

Optical principles of LC-OCT

LC-OCT is based on a combination optical coherence tomography (OCT) and reflectance confocal microscopy (RCM) with line illumination and line detection. Conventional OCT is a non-invasive optical imaging technique that generates vertical section image,[19] but whose resolution does not allow for imaging at the cellular level.[20] Like OCT, LC-OCT is fundamentally based on low-coherence interferometry (LCI). The principle of LCI is illustrated in Figure 1A. Light emitted by a broadband source is divided between the two arms of a Michelson-type interferometer. One arm (reference arm) schematically consists of a retro-reflector. The other arm (object arm) includes the object to be observed (the skin). In the object arm, light penetrates into the skin and is backscattered from the skin structures. Light reflected from the retro-reflector and backscattered from the skin are then recombined on a detector. This recombination yields interference if the difference between the optical path of the light from the two arms of the interferometer is less than the coherence length of the light source. The interference contains information about the amplitude of light backscattered by the skin structures located at a depth set by the position at which the optical path difference between the two arms is zero, with an axial resolution determined by the coherence length of the source. By scanning the length of the reference arm and applying appropriate data processing, the depth-profile of the backscattered light intensity can be retrieved from the interference.[21] LCI hence has the potential to generate in depth images with high axial resolution, provided the source has a broad enough spectrum.

In order to image with high lateral resolution, it is necessary for the interference signal to be acquired using an optical system with high lateral resolution. For this purpose, a high-resolution microscope objective can be placed in the object arm of the interferometer. The lateral resolution is ruled by the numerical aperture (NA) of the objective and the central wavelength of the light source spectrum. It should be noted that shorter wavelengths (towards blue light) lead to higher resolution, but also results in lower penetration into the skin. Conversely, longer wavelengths (towards red light) lead to lower resolution, but better penetration into the skin. For LC-OCT, a compromise between resolution and penetration was found by using 0.5 NA microscope objective with a supercontinuum laser[22] as the light source, centered at 800 nm (spanning from ~650 to 950 nm), resulting in a lateral resolution of the order of 1 μm and a penetration of 400-500 microns into the skin.

With the introduction of a microscope objective into the system, it is possible to arrange the illumination and detection so that the acquisition is performed in a confocal configuration, as in RCM. The principle of the confocal configuration is to illuminate a point in the sample (at the

Figure 1.—A) Schematic of an optical imaging system based on LCI; B) schematic of an optical imaging system combining LCI and confocal filtering.
BLS: broadband light source; OF: optical fiber; C: collimator; BS: cube beamsplitter, RR: retro-reflector; D: detector; MO: microscope objective; L: lens; P: pinhole; OPD: optical path difference.
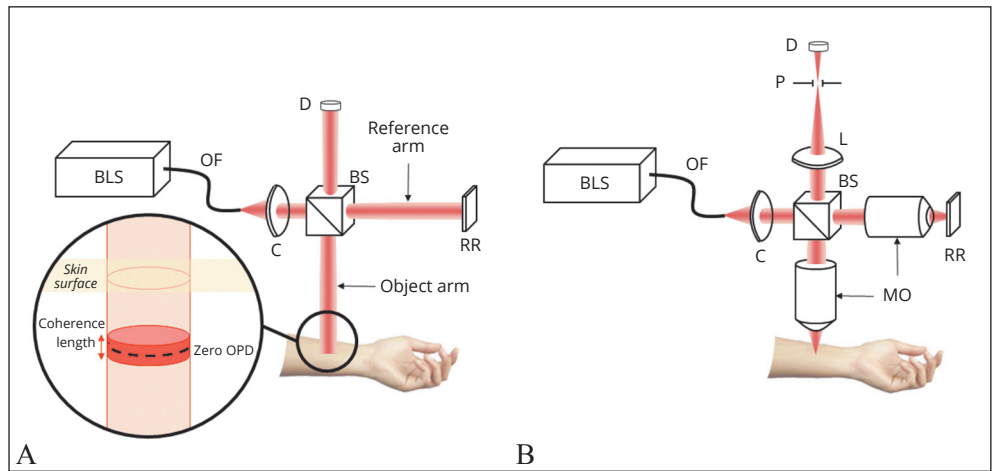
focus of the microscope objective), and to detect only the light backscattered from this point by spatially rejecting the light coming from outside the focus of the microscope objective, typically by positioning in front of the detector a pinhole conjugated with the focus of the microscope objective.[23] Such a confocal configuration significantly limits the amount of parasitic light reaching the detector, increasing the signal-to-noise ratio of the images.

In order to successfully combine the interferometric detection of OCT with the confocal filtering of RCM, it is necessary that the depth corresponding to zero optical path difference is identical to the depth at which the light is focused in the sample. Figure 1B illustrates the combination of LCI with a microscope objective in a confocal configuration (combination of OCT and RCM).

LC-OCT is based on an optical arrangement to illuminate the skin with a line of light and to detect the signal using a line-scan camera as the detector (Figure 2A). Line illumination is achieved by a cylindrical lens placed at the entrance of the interferometer. This configuration still maintains the confocal filtering, but only in one direction (a slit is used instead of a pinhole for filtering). Let us note that for LC-OCT, the array of pixels of the line-scan camera directly acts as a slit.

With line illumination and line detection, a single scan is sufficient for obtaining a two-dimensional image. A vertical image (perpendicular to the surface of the skin) is obtained by moving the whole interferometer axially using a piezoelectric stage, while a horizontal image (parallel to the surface of the skin) is obtained by scanning the line horizontally, using a galvanometer scanner placed in the object arm of the interferometer. In this mode, a piezoelectric chip generates a phase modulation as required in the data processing algorithm used to extract the interference signal amplitude.[10]

In order to obtain a color image of the skin surface in addition to the LC-OCT images, a separate imaging system was incorporated into the LC-OCT device. This system includes a ring of light emitting diodes (LEDs) positioned

Figure 2.—A) Experimental setup of LC-OCT; B) entire setup of LC-OCT integrating the surface imaging system.
BLS: broadband light source; OF: optical fiber; C: collimator; CL: cylindrical lens; BS: cube beamsplitter, RR: retro-reflector; MO: microscope objective; F: fold mirror; DF: dichroic filter; PS: piezoelectric stage; PC: piezoelectric chip; GS: galvanometer scanner; L: lens; LC: line-scan camera; LR: LED ring; AS: afocal system; CO: camera with micro-objective.
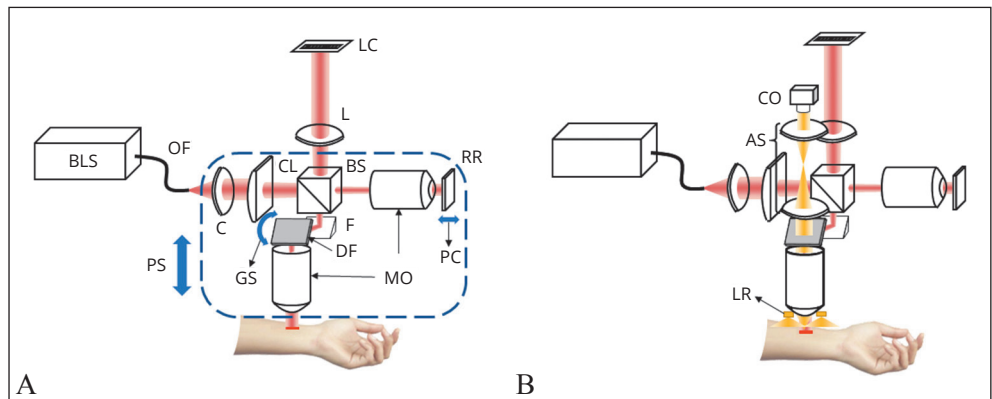
around the microscope objective for illuminating a large area of the skin with white light. A dichroic filter mounted on the galvanometer scanner separates the portion of the spectrum used for LC-OCT (reflected by the dichroic filter) and the portion of the spectrum used for surface imaging (transmitted by the dichroic filter). The light transmitted by the dichroic filter is collected by an afocal optical system, and sent towards a color area camera equipped with a micro-objective. To ensure that the image of the skin surface is always in focus, even when the LC-OCT line of light is scanned in the axial direction, the focus of the micro-objective is dynamically and automatically adjusted during image acquisition. The LC-OCT images and the images of the skin surface can thus be acquired simultaneously. Furthermore, the images are intrinsically co-localized as they are acquired simultaneously using the same microscope objective, allowing the location of the LC-OCT images to always be identified. Figure 2B shows the entire optical setup of LC-OCT integrating the surface imaging system.

Imaging modes and performance

LC-OCT offers three imaging modes: vertical mode, horizontal mode and 3D mode. The image of the skin surface is acquired in parallel to each of the three LC-OCT imaging modes, enabling precise localization of the area where LC-OCT images are acquired.

Vertical mode

Figure 3 shows a vertical LC-OCT image of healthy skin. The field of view of the image is 1.2×0.4 mm ($x \times z$). Both the axial resolution (in the z direction) and the lateral resolution (in the x direction) were measured to be 1.3 µm. The imaging speed is 8 frames per second, allowing video acquisition. The vertical image allows visualization of the upper layers and structures of the skin at cellular resolution, in a fashion similar to conventional histology. Stratum corneum, viable epidermis and dermis can be differentiated, with a clear dermal-epidermal junction (DEJ). Keratinocyte nuclei are clearly visible in the viable epidermis.

Horizontal mode

Figure 4 shows a horizontal LC-OCT image of healthy skin acquired at the level of the epidermis (stratum spinosum). The field of view of the image is 1.2×0.5 mm ($x \times y$). The resolution (both in the x and y directions) was measured to be 1.3 µm. As for the vertical mode, the imaging

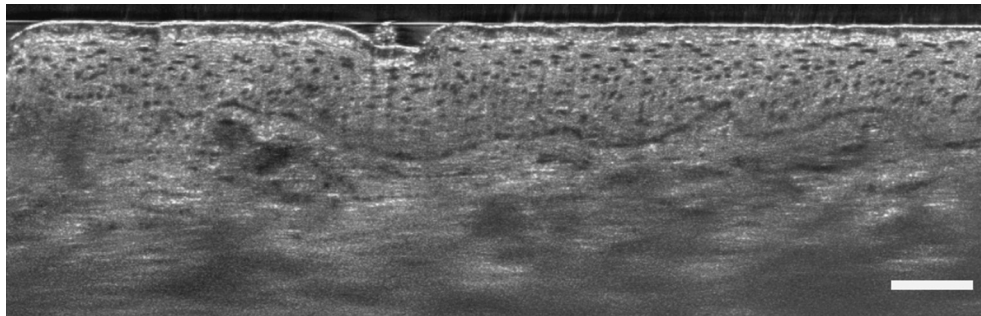Figure 3.—Vertical LC-OCT image of healthy skin. Scale bar: 100 µm.
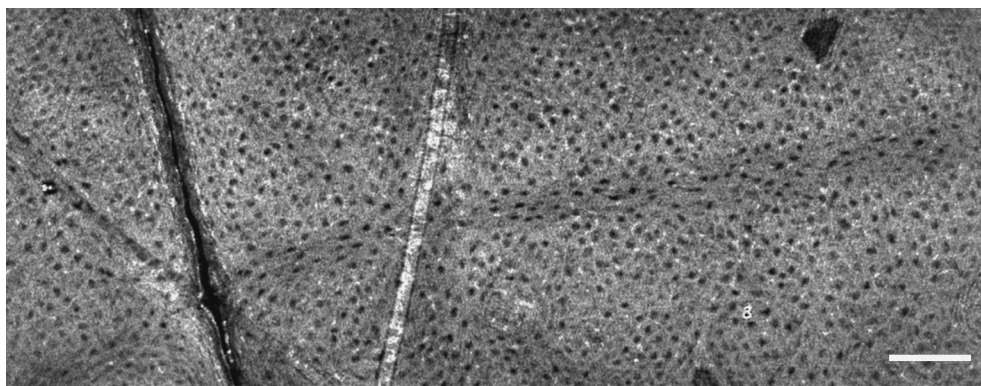

Figure 4.—Horizontal LC-OCT image of healthy skin. Scale bar: 100 µm.

speed is 8 frames per second, allowing video acquisition. The keratinocyte nuclei and the honeycomb architecture of the keratinocytes can be clearly visualized.

3D mode

Three-dimensional (3D) images are obtained by stacking horizontal images, with a 1 µm step in the axial direction between consecutive images. The field of view of the resulting 3D image can be up to $1.2 \times 0.5 \times 0.5$ mm ($x \times y \times z$), with an isotropic resolution of 1.3 µm. In this mode, the horizontal images used for reconstructing the 3D image

are acquired at a speed of 20 frames per second, resulting in a duration of 25 s for acquisition of the full accessible field of view. Figure 5 shows a 3D LC-OCT image of healthy skin. The volume-rendering visualization makes it possible to observe the three-dimensional architecture and connections of the structures in the skin at cellular level, which is not accessible by conventional histology.

Surface image

Figure 6 shows the surface image associated to the three-dimensional image of healthy skin previously shown. The
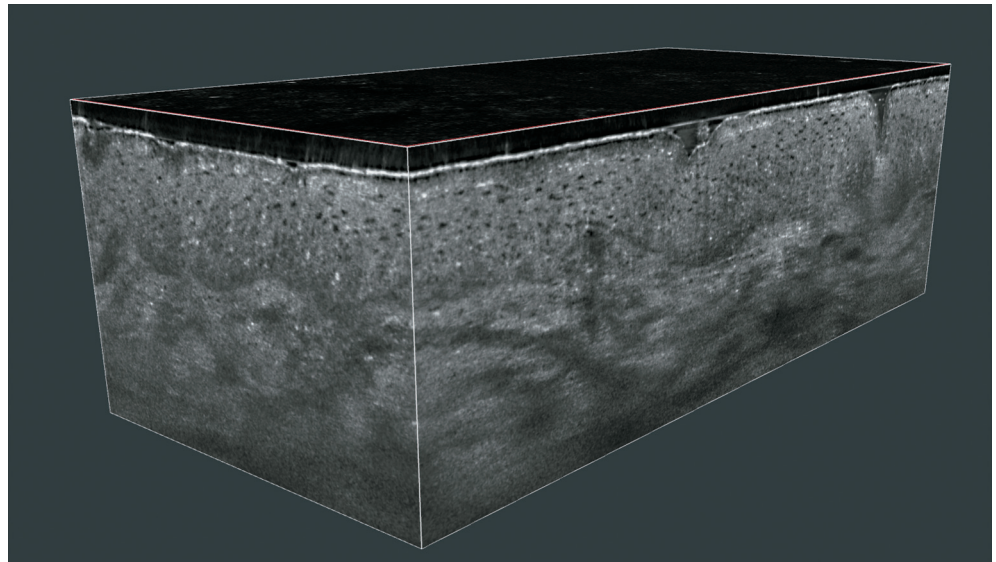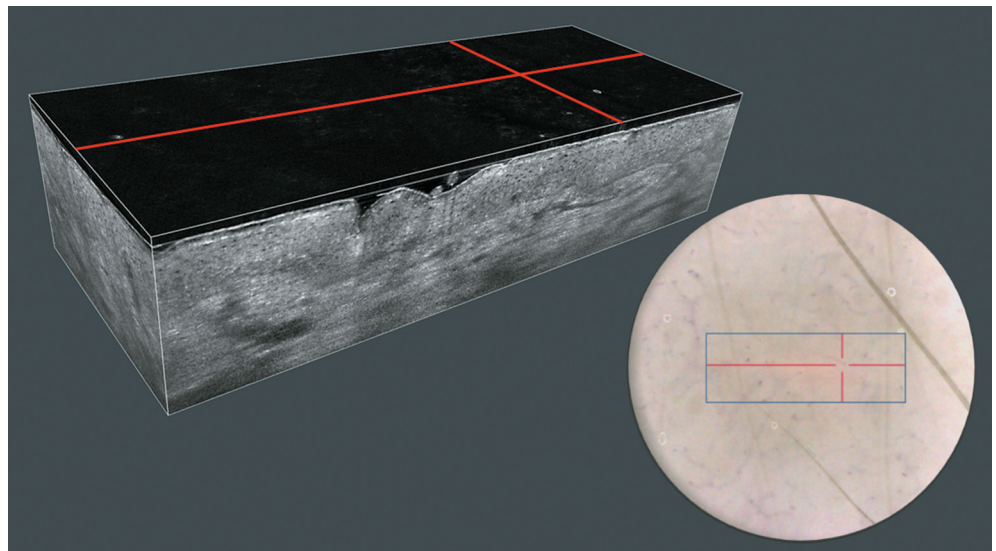
Figure 5.—3D LC-OCT image of healthy skin.

Figure 6.—Surface image of healthy skin (right) and its associated 3D LC-OCT image (left). The blue rectangle indicates the position of acquisition of the LC-OCT image. The reticle appears in red.

field of view of the image is a disk of diameter 2.6 mm. The resolution of 5 μm of the surface image enables the observation of the same features as in conventional dermoscopy, and therefore provides a direct link between the LC-OCT examination and the dermoscopic examination. The LC-OCT images can thus be acquired in regions of interest identified with dermoscopy. On the surface image, a marker indicates the position of acquisition of the LC-OCT images: a red line in the vertical mode, a blue rectangle in the horizontal and 3D modes, allowing easy positioning by the user. When reviewing the LC-OCT images, a reticle allows the user to associate a point in the LC-OCT images to a point in the associated surface images.

Practical use of LC-OCT

The LC-OCT optical setup can be compacted enough to be integrated inside a handheld probe. Figure 7A shows the LC-OCT probe developed by DAMAE Medical (deepLive™), integrating the three imaging modes previously described. The probe weighs less than 1.2 kg, and can be easily positioned on any parts of the body. A drop of paraffin oil must be placed onto the skin before imaging, in order to ensure the optical contact between the probe and the skin. The probe is linked to a small footprint central unit mounted on a standard medical cart. Figure 7B shows the full deepLive™ system.

DAMAE Medical has developed a user-friendly software that allows the acquisition of LC-OCT images and their intuitive storage in patient files. A patient file can be created in less than 1 minute by registering his/her demographic information (first name, last name, date of birth, skin phototype, gender, hospital ID) and designating the precise lesion location on a designed body mapper.

After applying a drop of paraffin oil on the lesion, the probe is gently pressed against the skin. The surface image serves first to target the lesion, then its role is to guide the examination and ensure the sufficient coverage of the lesion. Despite the fact that the extent of skin lesions generally exceeds the field of view of LC-OCT, the real-time image acquisitions in the vertical and horizontal modes at 8 frames per second combined with the guiding surface image allows for easy and fast coverage of the entire lesion.

A button on the handle of the probe is used to start recording images and to switch between the different imaging modes. Another button allows the user to adjust the position of acquisition in the vertical mode or the depth of imaging in the horizontal mode, with a 1 μm precision.

The recommended imaging acquisition protocol depends on the expected nature of the lesion. The vertical mode is well-suited to assess the presence of lobular structures and their position relative to the epidermis (connected or separated), the appearance of the dermo-epidermal junction (preserved or destroyed), and the position of cellular atypia in the epidermis (near the basal layer or in pagetoid ascent). Conversely, the horizontal mode is more effective in analyzing the regularity of the keratinocyte network or revealing the presence of dendritic cells, which are preferentially distributed in a horizontal plane parallel to the skin surface. Therefore, the vertical mode is primar-

Figure 7.—A) DeepLive™ LC-OCT probe used on a patient; B) full deepLive™ system.

ily used for diagnosing basal cell carcinomas (BCCs), actinic keratoses (AKs), squamous cell carcinomas (SCCs), or inflammatory lesions, while the 3D mode is preferred for atypical melanocytic lesions, as both vertical and horizontal analyses provide complementary information.

Typically, the examination of a patient using deep-Live™ and the previously described workflow lasts between 5 and 10 minutes.

After examination, LC-OCT images with their associated surface images can be reviewed using deepLive™ software. 3D images can be displayable according to two different views: simultaneous XZ and XY planes or volume-rendering. For specific needs, various custom image processing algorithms are available to facilitate image review and analysis.

Additionally, deepLive™ software allows for the registration of clinical suspicions, LC-OCT diagnosis, patient management, and histological diagnosis to facilitate patient follow-up. The architecture of the patient database makes it possible to find an existing patient and add an additional lesion, or add a follow-up examination on a pre-existing lesion.

Artificial intelligence algorithms for LC-OCT image analysis

Owing to the real-time and 3D imaging capabilities of LC-OCT, automated deep learning algorithms can be particularly useful in the analysis of LC-OCT images. The use of deep learning algorithms can save a significant amount of time in terms of annotations and review for medical doctors and can perform tasks that cannot be done manually in a reasonable time.

DAMAE Medical has developed several deep learning algorithms, in particular for the segmentation of skin layers and keratinocyte nuclei. These algorithms enable the automatic segmentation of the different skin layers imaged by LC-OCT (stratum corneum, viable epidermis and dermis) in both vertical mode and 3D mode. The segmentation of the viable epidermis and dermis yields a segmentation of the DEJ. Moreover, the segmentation of keratinocyte nuclei in a 3D LC-OCT image can be performed using StarDist algorithm[24] in less than two minutes, whereas it is infeasible by hand since a single 3D LC-OCT image can count more than 40,000 cells. Figure 8 shows an example
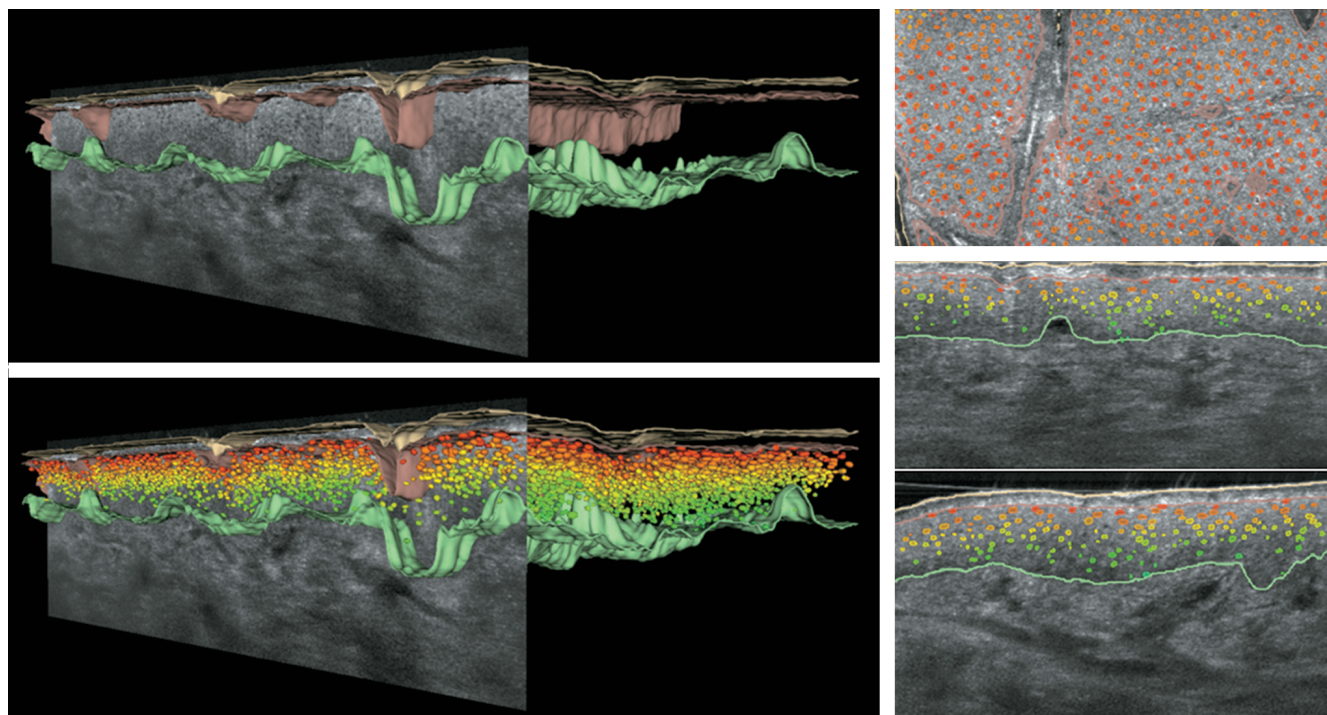

Figure 8.—Deep-learning segmentation algorithms applied to a 3D LC-OCT image of healthy skin (top left and bottom left). The segmentation of the interface between the different skin layers is displayed (yellow = skin surface, brown = interface between stratum corneum and viable epidermis, green = DEJ). The segmentation of the keratinocyte nuclei is also displayed, with a color coding depending on their volume (green = smaller nuclei, red = larger nuclei). The segmentations are also shown on cuts along three different planes: XY (top right), XZ (middle right), YZ (bottom right).

of segmentation of both the skin layers and the keratinocyte nuclei applied to the 3D LC-OCT image shown in Figure 5.

The segmentation algorithms provide accurate and reproducible metrics that can be used to evaluate or monitor a lesion. In Chauvel-Picard *et al.*,[25] a set of epidermal metrics (epidermal thicknesses, DEJ undulation and keratinocyte number/shape/size) were computed from segmented images obtained from eight female volunteers in order to quantify healthy skin across seven different body sites. The output segmentations can also be used as inputs for other algorithms as shown in Fischman *et al.*[26] where cellular atypia was quantified at super-human level of performance by giving 13 physically-sound metrics to an XG-Boost model[27] trained in a semi-supervised approach. This algorithm was demonstrated to have the potential to grade pre-cancerous keratinocytic lesions.

Conclusions

LC-OCT is one of the most promising techniques for "*in vivo* histology" of the skin, presenting a great interest for the early diagnosis and therapeutic monitoring of numerous skin diseases. In the form of a handheld probe, the deepLive™ device developed by DAMAE Medical offers easy access to almost all parts of the skin, and is of convenient use by dermatologists. LC-OCT provides cellular resolution and real-time imaging capabilities, along with the possibility to generate either vertical, horizontal or 3D images associated with a dermoscopy-like surface image acquired in parallel. LC-OCT images have an accessible field of view of ~1.2 × 0.5 × 0.5 mm ($x \times y \times z$). The real-time acquisition is made possible by a line-field arrangement, yielding an acquisition speed of 8 frames per second for the vertical and horizontal modes, and acquisitions in less than 25 s for the 3D mode. The dermoscopic resolution of the surface images (5 μm) allows practitioners to easily locate where to acquire LC-OCT images based on dermoscopic examination. An efficient workflow has been developed and implemented in the software associated to deepLive™ for easy usage in clinical routine, with examination durations generally less than 10 minutes and easy patient management for follow-up examinations. Eventually, as LC-OCT can generate a large amount of data, automated deep learning algorithms have been developed, allowing practitioners to save considerable time in terms of review and annotation. These algorithms can also help in the interpretation of the images.

References

1. Tognetti L, Fiorani D, Tonini G, Zuliani L, Cataldo G, Balistreri A, *et al.* Dermoscopy: Fundamentals and Technology Advances. Technology in Practical Dermatology. 2020; 3–24.

2. Kittler H, Pehamberger H, Wolff K, Binder M. Diagnostic accuracy of dermoscopy. Lancet Oncol 2002;3:159–65.

3. Nehal KS, Gareau D, Rajadhyaksha M. Skin imaging with reflectance confocal microscopy. Semin Cutan Med Surg 2008;27:37–43.

4. Pellacani G, Farnetani F, Ciardo S, Chester J, Kaleci S, Mazzoni L, *et al.* Effect of Reflectance Confocal Microscopy for Suspect Lesions on Diagnostic Accuracy in Melanoma: A Randomized Clinical Trial. JAMA Dermatol 2022;158:754–61.

5. Kadouch DJ, Leeflang MM, Elshot YS, Longo C, Ulrich M, van der Wal AC, *et al.* Diagnostic accuracy of confocal microscopy imaging vs. punch biopsy for diagnosing and subtyping basal cell carcinoma. J Eur Acad Dermatol Venereol 2017;31:1641–8.

6. Rajadhyaksha M, Marghoob A, Rossi A, Halpern AC, Nehal KS. Reflectance confocal microscopy of skin in vivo: from bench to bedside. Lasers Surg Med 2017;49:7–19.

7. Encabo B, Segurado G, González S. History and Fundamentals of Reflectance Confocal Microscopy. Technology in Practical Dermatology. 2020; 127–134.

8. Dubois A, Levecq O, Azimani H, Siret D, Barut A, Suppa M, *et al.* Line-field confocal optical coherence tomography for high-resolution noninvasive imaging of skin tumors. J Biomed Opt 2018;23:1–9.

9. Ruini C, Schuh S, Sattler E, Welzel J. Line-field confocal optical coherence tomography-Practical applications in dermatology and comparison with established imaging methods. Skin Res Technol 2021;27:340–52.

10. Ogien J, Levecq O, Azimani H, Dubois A. Dual-mode line-field confocal optical coherence tomography for ultrahigh-resolution vertical and horizontal section imaging of human skin in vivo. Biomed Opt Express 2020;11:1327–35.

11. Ogien J, Daures A, Cazalas M, Perrot JL, Dubois A. Line-field confocal optical coherence tomography for three-dimensional skin imaging. Front Optoelectron 2020;13:381–92.

12. Ogien J, Levecq O, Cazalas M, Suppa M, del Marmol V, Malvehy J, *et al.* Handheld line-field confocal optical coherence tomography for dermatology. In: Proceedings of Photonics in Dermatology and Plastic Surgery. San Francisco; 2020.

13. Ogien J, Waszczuk L, Suppa M, Del Marmol V, Malvehy J, Cinotti E, *et al.* Optical skin biopsy using multimodal line-field confocal optical coherence tomography (LC-OCT). In: Proceedings SPIE 11948. XXVI Conference of Optical Coherence Tomography and Coherence Domain Optical Methods in Biomedicine; 2022.

14. Suppa M, Fontaine M, Dejonckheere G, Cinotti E, Yélamos O, Diet G, *et al.* Line-field confocal optical coherence tomography of basal cell carcinoma: a descriptive study. J Eur Acad Dermatol Venereol 2021;35:1099–110.

15. Ruini C, Schuh S, Gust C, Kendziora B, Frommherz L, French LE, *et al.* Line-field optical coherence tomography: in vivo diagnosis of basal cell carcinoma subtypes compared with histopathology. Clin Exp Dermatol 2021;46:1471–81.

16. Ruini C, Schuh S, Gust C, Kendziora B, Frommherz L, French LE, *et al.* Line-field confocal optical coherence tomography for the in vivo real-time diagnosis of different stages of keratinocyte skin cancer: a preliminary study. J Eur Acad Dermatol Venereol 2021;35:2388–97.

17. Perez-Anker J, Puig S, Alos L, García A, Alejo B, Cinotti E, *et al.* Morphological evaluation of melanocytic lesions with three-dimensional line-field confocal optical coherence tomography: correlation with histopathology and reflectance confocal microscopy. A pilot study. Clin Exp Dermatol 2022;47:2222–33.

18. Cinotti E, Brunetti T, Cartocci A, Tognetti L, Suppa M, Malvehy J, *et al.* Diagnostic Accuracy of Line-Field Confocal Optical Coherence

Tomography for the Diagnosis of Skin Carcinomas. Diagnostics (Basel) 2023;13:361.

19. Huang D, Swanson EA, Lin CP, Schuman JS, Stinson WG, Chang W, *et al.* Optical coherence tomography. Science 1991;254:1178–81.

20. Welzel J. Optical coherence tomography in dermatology: a review. Skin Res Technol 2001;7:1–9.

21. Larkin KG. Efficient nonlinear algorithm for envelope detection in white light interferometry. J Opt Soc Am A Opt Image Sci Vis 1996;13:832–43.

22. Granzow N. Supercontinuum white light lasers: a review on technology and applications. In: Proceedings of the Joint TC1—TC2 International Symposium on Photonics and Education in Measurement Science. Jena, Germany; 17-19 September 2019.

23. Minsky M. Microscopy apparatus. U.S. Patent 3013467; 1961.

24. Weigert M, Schmidt U, Haase R, Sugawara K, Myers G. Star-convex Polyhedra for 3D Object Detection and Segmentation in Microscopy. 2020 IEEE Winter Conference on Applications of Computer Vision (WACV); 2020.

25. Chauvel-Picard J, Bérot V, Tognetti L, Orte Cano C, Fontaine M, Lenoir C, *et al.* Line-field confocal optical coherence tomography as a tool for three-dimensional in vivo quantification of healthy epidermis: A pilot study. J Biophotonics 2022;15:e202100236.

26. Fischman S, Pérez-Anker J, Tognetti L, Di Naro A, Suppa M, Cinotti E, *et al.* Non-invasive scoring of cellular atypia in keratinocyte cancers in 3D LC-OCT images using Deep Learning. Sci Rep 2022;12:481.

27. Chen T, Guestrin C. XGBoost: A Scalable Tree Boosting System. In: Proceedings of the 22nd ACM SIGKDD International Conference on Knowledge Discovery and Data Mining; 2016.